

A universal route from avalanches in mean-field models with random fields to stochastic Poisson branching events.

Jordi Baró

*Departament de Física de la Materia Condensada,
Universitat de Barcelona, 08028 Barcelona, Spain
Universitat de Barcelona Institute of Complex Systems (UBICS),
Universitat de Barcelona, 08028 Barcelona, Spain and
Centre de Recerca Matemàtica, Edifici C, Campus Bellaterra, E-08193 Barcelona, Spain*

Álvaro Corral

*Departament de Matemàtiques, Facultat de Ciències,
Universitat Autònoma de Barcelona, E-08193 Barcelona, Spain
Centre de Recerca Matemàtica, Edifici C, Campus Bellaterra, E-08193 Barcelona, Spain and
Complexity Science Hub Vienna, Josefstädter Straße 39, 1080 Vienna, Austria*

Avalanches in mean-field models can be mapped to memoryless branching processes defining a universality class. We present a reduced expression mapping a broad family of critical and subcritical avalanches in mean-field models at the thermodynamic limit to rooted trees in a memoryless Poisson branching processes with random occurrence times. We derive the exact mapping for the athermal random field Ising model and the democratic fiber bundle model, where avalanche statistics progress towards criticality, and as an approximation for the self-organized criticality in slip mean-field theory. Avalanche dynamics and statistics in the three models differ only on the evolution of the field density, interaction strength, and the product of both terms determining the branching number.

Many complex systems with discrete symmetry breaking exhibit *avalanche dynamics*. Under quasistatically slow external driving, the temporal evolution $v(t)$ of physical observables appears to be split between long periods of quiescence and well-delimited fast transformation events, the so-called *avalanches*. Due to their fast nature, such avalanches can be regarded as instantaneous and labeled as point events k in time with a defined time origin t_k , and marked by their magnitude or size $S_k = \int_{t_k}^{t_k+T_k} v(t)dt$, and by the duration T_k of the excursion out of quiescence, which models the dynamics of the system. Many physical systems exhibit criticality in the form of scale-free avalanches [1–4] rendering power-law distributions of sizes and durations.

The cascading nature of avalanches has long been associated with branching processes [4–10] where each element i in a generation g triggers a number $Y_{i,g} = 0, 1, 2..$ of new elements forming part of generation $g + 1$. The total number of offspring in each generation g as given by $Z_g = \sum_{i=1}^{Z_{g-1}} Y_{i,g-1}$, imposing $Z_0 = 1$. Avalanche sizes (S) are analogous to the sizes of extinguished rooted trees $\Delta := \sum_{g=0}^{G-1} Z_g$, after a number of generations, or *depth*, G , analogous to durations (T), such that $Z_{G-1} > 0$ and $Z_G = 0$. We focus on those processes, customarily designated to belong to the mean field (MF) universality class (MF-UC), where avalanche propagation can be mapped to memoryless, a.k.a. Galton-Watson, branching processes [5–7] where all $Y_{i,g}$ are i.i.d. (independent and identically distributed). We highlight the properties of memoryless branching constituting the MF-UC:

(i) The expected number of elements in generation g reads $E(Z_g) = E(Y)^g = \mu^g$, where $\mu := E(Y)$ is the

branching parameter. Then, the expected tree size is:

$$E(\Delta) = \sum_{g=0}^{\infty} E(Z_g) = \sum_{g=0}^{\infty} \mu^g = \frac{1}{1-\mu}, \quad (1)$$

for $\mu \leq 1$, whereas $E(\Delta) \rightarrow \infty$ for $\mu \geq 1$.

(ii) For any offspring distribution with well-defined statistical moments and at criticality (that is, for $\mu = 1$), the survival probability beyond generational depths G is asymptotically $P(G_k > G) \propto G^{-1}$, rendering a probabilistic mass function (p.m.f.) of avalanche depths [11]:

$$pmf_G(G) \sim G^{-\kappa_G} \quad \text{with } \kappa_G = 2. \quad (2)$$

(iii) Close to criticality [12, 13], the size of such extinguished rooted trees (Δ), is linked to characteristic avalanche depths, e.g., G , in a relation of the type:

$$E(G|\Delta) \sim \Delta^\gamma \quad \text{with } \gamma = 0.5, \quad (3)$$

leading to the critical size distribution:

$$pmf_\Delta(\Delta) \sim \Delta^{-\kappa_\Delta} \quad \text{with } \kappa_\Delta = 1 + \gamma(\kappa_G - 1) = 3/2. \quad (4)$$

These memoryless branching (from now on MF) exponents, are ubiquitous in natural avalanche process close to criticality [14–17] and are reproduced by MF models [1, 5–7, 18–21]. As a paradigmatic example, sand-pile models with random grain redistribution rules leading to self-organized criticality (SOC) have traditionally been modeled as binomial branching processes [1, 7, 18]. In this Letter we identify another category of avalanche models which maps to a Poisson branching process. Inspired by early results by Sethna et al. [20] we derive

a universal route to Poisson branching processes from (i) the mean-field *random field Ising model* (RFIM) and prove its validity for two other prototypical models: (ii) *the democratic fiber bundle model* (DFBM) [19, 22], and (iii) *slip mean-field theory* (SMFT) [21].

i) Tunable branching in the random field Ising model:

Let us write the Hamiltonian of a system of N spins with value $s_i = \{-1, +1\}$, and all-to-all ferromagnetic ($J > 0$) interactions in reduced units as:

$$\mathcal{H}(t) = - \sum_{i=1}^N s_i(\xi(t) - h_i), \quad (5)$$

where the quenched disordered fields h_i uniquely felt by each spin i are i.i.d. given a probability density $\rho_h(h_i = \xi')d\xi'$. The global term, or *mean field*, $\xi(t)$ is the same for all spins and is given by a linear combination of the external driving field $H(t)$ and the interaction with all other spins s_j approximated as $\frac{J}{N} \sum_{j \neq i} s_j \approx \frac{J}{N} \sum_j s_j =: Jm$, a.k.a. the magnetization field, such that:

$$\xi(t) := H(t) + Jm(t). \quad (6)$$

Under athermal conditions, $\mathcal{H}(t)$ minimizes locally by setting each spin as $s_i = \text{sign}[\xi(t) - h_i]$. Considering a monotonic driving $\dot{H} > 0$ from an original configuration $\{s_i\} = \{-1\}$, each spin flips on the condition: $h_i < \xi(t)$. Therefore, $m = m(\xi)$ since it is proportional to the number of spins with $h_i > \xi$. This intrinsic relation potentially leads to an indeterminate m above a critical density $\rho_h(\xi) > (2J)^{-1} := \rho_c(J)$ [20] (see Fig. 3.a). The stochastic $\{h_i\}$ introduces shorter indeterminate intervals below ρ_c (Fig. 3.b), corresponding to avalanches.

Inspired by the study of avalanches in the RFIM and random transport [20, 23], we construct here a general model consisting of a sorted set of random thresholds $\{..X_i < X_{i+1}..\}$, e.g. random fields h_i in the RFIM, and a mean field $\xi(t)$ defining the state of the system as:

$$\xi(t) := \mathcal{B}(t) + \sum_{i|X_i < \xi(t)} \mathcal{R}_i(t - t_i), \quad (7)$$

that is, a linear combination of a monotonic external driving term $\mathcal{B}(t)$ and monotonic responses $\mathcal{R}_i(\tau)$ caused by each activated threshold. The activation time of each threshold (t_i) is the instant when the increasing field $\xi(t)$ crosses the threshold X_i assuming $\mathcal{R}_i(\tau < 0) = 0$.

The nonlinear coupling between ξ and $\mathcal{R}_i(\tau)$ gives rise to avalanches. If the driving is quasistatically slow compared to the response $\dot{\mathcal{B}} \ll \dot{\mathcal{R}}_i$, avalanches are well defined in time as concatenated responses $\{\mathcal{R}_i\}$ which we can consider to be instantaneous, such that:

$$\mathcal{R}_i(\tau) = l_i \Theta(\tau - \delta_g), \quad (8)$$

after an infinitesimal delay time δ_g clustering field steps in discretized generations, a.k.a. shells, g within the

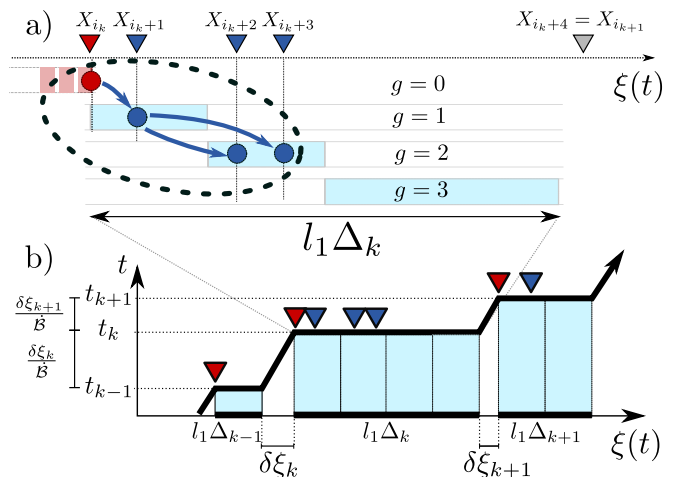


FIG. 1: (a) One avalanche represented as a branching process within (b) an avalanche sequence represented as a point process in field ξ and time t considering constant driving rate $\dot{\mathcal{B}}$. Red triangles represent the values of thresholds (i_j) triggering each avalanche j when $\xi(t_j) = X_{i_j}$. Blue triangles represent thresholds activated within the avalanche propagation. Blue rectangles of length $Z_g l_1$ represent the interval of instant transformation at each shell $g+1$ leading to the activation of Z_{g+1} thresholds $\{X_i\}$. Blue arrows represent causal connection, i.e., branching, between activations (circles).

avalanche. Here, $\Theta(x)$ is the step function defined as $\Theta(x) = 0$ for $x \leq 0$ and $\Theta(x) = 1$ for $x > 0$. The factor l_i is a characteristic field increase in units of ξ . The stochastic nature of avalanches derives from the i.i.d. $\{X\}$, with an expected number ν , a.k.a. density, of thresholds per unit of field (ξ). The match between the RFIM and the model defined by Eqs. (7) and (8) is directly given by:

$$l_i \equiv \frac{2J}{N}; \dot{\mathcal{B}}(t) \equiv \dot{H}(t); \{X_i\} \equiv \{h_i\}, \quad (9)$$

Finite avalanches themselves are too small to modify the state $\xi(t)$ of infinite systems. By considering that $\nu(\xi)$ and $l_i(\xi)$ are, at most, function of state, these can be approximated as constants during intervals of avalanche sequences. Such infinitesimal intervals of ξ variation can be mapped onto a stochastic point process with stationary laws, as illustrated in Fig. 1.b. Avalanches are well identified sudden advancements of $\xi(t)$, separated by i.i.d. time intervals of width $\delta\xi_k/\dot{\mathcal{B}}$, with $\delta\xi_k$ the change in $\xi(t)$ between the end of the $k-1$ -th avalanche and the beginning of the k -th. The size and duration marking the event is determined by the propagation profile between the nucleation and halting of an avalanche, as illustrated for avalanche k in Fig. 1.a. The avalanche is triggered through quasistatic driving $\dot{\mathcal{B}}(t) > 0$ when $\xi(t)$ reaches the threshold value of the element X_{k_0} nucleating the avalanche k at an instant $t_{k,0}$. Since we consider the immediate response approximation (8), the external field $\mathcal{B}(t)$ will remain constant during the propagation of the avalanche. The variation of ξ from $t_{k,0}$ to $t_{k,1} = t_{k,0} + \delta$ reads $\xi(t_1) = \xi(t_0) + l_1$, crossing a number $Z_{k,1}$ of con-

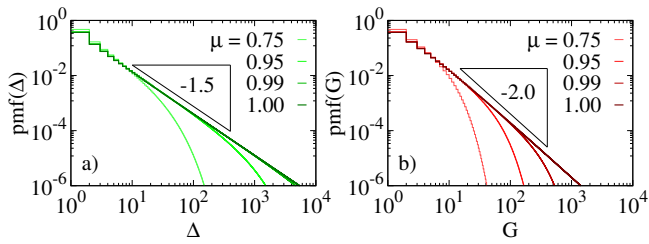


FIG. 2: Exact local distributions of (a) sizes and (b) durations given by (11) and (12) valid for any model represented by (7).

secutive thresholds $\{X_{k_0+1}, \dots, X_{k_0+Z_{k,1}}\}$, which will constitute the shell, or generation, $g = 1$ of event k . Since X_i are i.i.d. and homogeneous, the number of “offspring thresholds” activated within the interval $\Delta\xi = l_1$ is a Poisson number with parameter:

$$\mu := E(Z_{k,1}) \equiv E(Y) = \nu \times l_1. \quad (10)$$

In its turn, the activation of the $Z_{k,1}$ thresholds will advance $\xi(t)$ over the next instant: $\xi(t_{k,2} = t_{k,0} + 2\delta) = \xi(t_{k,1}) + Z_{k,1}l_1$ which will cross a Poisson number $Z_{k,2}$, with $E(Z_{k,2}) = Z_{k,1}\mu$, of thresholds $\{X_{k_0+Z_{k,1}+1}, \dots, X_{k_0+Z_{k,1}+Z_{k,2}}\}$ that comprise the shell $g = 2$. The process stops when $Z_{k,G} = 0$, resulting in an avalanche of size $\Delta_k := 1 + \sum_g Z_{k,g}$ with a corresponding increase in field $\xi(t_{k,G}) = \xi(t_{k,0}) + \Delta_k l_1$ and lasting a time $T_k = G_k \delta_g$. As described, the propagation of the avalanche is equivalent to a memoryless Poisson branching process with a branching ratio μ . Subcritical ($\mu < 1$) avalanche sizes (Δ) are equivalent to subcritical Poisson tree sizes, which are i.i.d. according to a Borel distribution [13, 24]:

$$pmf_{\Delta}(\Delta; \mu) = \frac{(\mu\Delta)^{\Delta-1} e^{-\mu\Delta}}{\Delta!}, \quad (11)$$

with $\Delta = 1, 2, \dots$; Moreover, avalanche survival after G generations is given by the self-recurrent expression [24]:

$$P_G(g; \mu) = 1 - e^{-\mu P_G(g-1; \mu)} \quad ; \quad P_G(0; \mu) = 1. \quad (12)$$

As shown in Fig. 2, for large Δ and G and close to $\mu \sim 1$, these expressions can be numerically approximated by the universal forms (2) and (4). The maximum likelihood estimation for μ from (11) corresponds to (1):

$$\hat{\mu} = 1 - \langle \Delta \rangle^{-1}, \quad (13)$$

with $\langle \Delta \rangle$ the sample mean of the avalanche size, and with the uncertainty given by the Fisher information: $\widehat{\sigma}_{\mu}^2 = \mu(1 - \mu)/N$.

We remark that the dynamics and statistics of avalanches are fully determined by only two terms: (i) the density of random thresholds (ν) determining the rate of avalanches in units of ξ ; (ii) the step size (l_i) converting branching numbers into units of ξ . Given constant

l_1 and ν , the resulting avalanche sequence can be exactly modeled as an homogeneous point process in the ξ axis (x -axis in Fig. 1.b) with dead-times $l_1 \Delta_k$ being the sizes Δ_k i.i.d. Borel distributed with parameter μ (10). Considering a slow driving rate $\dot{\mathcal{B}}$, the dead times are negligible, recovering a standard Poisson process in time (y -axis in Fig. 1.b).

The representation in (7) is valid in general for non-stationary $\{l_1, \nu\}(\xi)$ at the thermodynamic limit, potentially leading to a divergence of susceptibilities at $\mu = 1$ with a corresponding third independent exponent. E.g., Fig. 3.a-c, show transitions between different avalanche regimes in the RFIM given the same non-uniform $\nu(\xi)$ from a Gaussian distribution, and different values of J . Sizes diverge at criticality ($\mu = 1$) matching the global instability limit at $\rho_c(J)$, before entering supercritical regimes which are out of the scope of this Letter.

ii) Critical failure in fiber bundle models: The *democratic fiber bundle model* (DFBM) is a prototype model of so-called critical failure [19, 22], meaning that, as the driving progresses, avalanche statistics exhibit a monotonic evolution towards and beyond criticality, $\mu = 1$ in terms of (7), causing a catastrophic failure or instability. The DFBM simulates the deformation and resilience of an ensemble of brittle elastic elements, a.k.a. fibers, plugged in parallel and sustaining an increasing load. Each fiber fails under stress driving when the local stress σ_l exceeds a random strength s_i , which is i.i.d. given a density $\nu(\sigma_l) := \frac{dn}{d\sigma_l}$. The total tension ($F(t)$) is equally sustained by the number of unbroken fibers $n(t)$. Therefore, the local stress for each fiber reads $\sigma_l(t) = F(t)/n(t)$. Assuming a monotonous driving in $F(t)$, $n(t)$ is the number of fibers $\{i\}$ with $s_i > \sigma_l(t)$. It is then convenient to redefine $n(\sigma_l) := n(t|s_i > \sigma_l(t)) = \int_{\sigma_l(t)}^{\infty} \nu(s') ds'$. The mechanical stability of the bundle is defined by the constitutive equation:

$$\sigma_l = \frac{F}{n(\sigma_l)}. \quad (14)$$

Under force driving, (14) displays a singular instability at the failure point $\sigma_{l,f} = n(\sigma_{l,f})/\nu(\sigma_{l,f})$, or $F_f = n(\sigma_{l,f})\sigma_{l,f}$, above which the bundle fails catastrophically (see Fig. 3.d). Defining the mean field as $\xi(t) \equiv \sigma_l(t)$, and considering large system sizes such that $n \approx n - 1$, (14) can be rewritten as the sum of the driving intervals and the steps $\sum_i [\sigma_l(t_i + \delta t) - \sigma_l(t_i)]$ caused by fibers breaking on the thresholding $\sigma_l > s_i$, leading to a form equivalent to (7) with terms:

$$l_i \equiv \frac{F(t_i)}{[n(t_i)]^2}; \quad \dot{\mathcal{B}}(t) \equiv \frac{\dot{F}(t)}{n(t)}; \quad \{X_i\} \equiv \{s_i\}. \quad (15)$$

In the DFBM, l_i and $\dot{\mathcal{B}}$ are non-stationary and depend on the state of the fracture process. In particular, we observe a mild increase in the activity over time, and the failure point $(\sigma_{l,f}, F_f)$ coincides with the

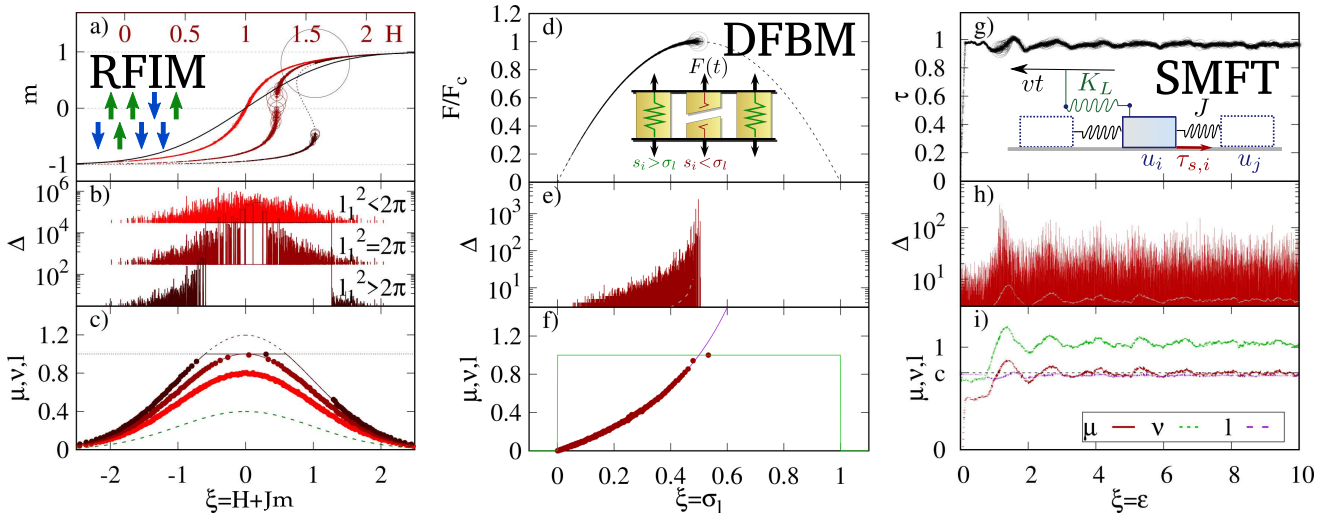


FIG. 3: Numerical simulations and evolution of parameters in terms of the mean field ξ : (a-c) Three RFIM with $N = 5 \times 10^4$ spins and subcritical ($J = l_1/2 = 1$), critical ($J = \sqrt{\pi}/2$) and supercritical ($J = 1.5$) Gaussian disorder field; (d-f) a DFBM of $n(0) = 5 \times 10^5$ with uniform distribution of strengths; and (g-i) a SMFT with $N = 10^5$ and a broad uniform distribution of disorder ($\tau_{s,i} \in (0.675, 1.325)$) and $c = 0.75$. Top row shows the evolution of the traditional order parameters. An additional x-axis has been added to (a) to show the dependence in terms of external field H for different values of disorder (red lines colorcoded as (b)). Middle row shows the sequence of avalanche sizes ($\Delta > 3$). Bottom rows show the selected (c,f) and emergent (i) density ν of the thresholds, l_1 (constant and eluded in c) and the estimated $\hat{\mu}$ (13) using 1000 avalanches.

critical branching ratio $\mu_f = \sigma_{l,f} \nu(\sigma_{l,f}) / n(\sigma_{l,f}) = 1$ (Fig. 3.f), reached after a monotonic increase in μ . This equivalence between failure and avalanche criticality exposed through (7) vindicates the use of raw avalanche statistics, e.g., acoustic monitoring, to predict failure [17, 25–29]. Below F_f , fibers fail in subcritical bursts, following a Poisson branching process with Borel i.i.d. sizes (11) for $\mu(\sigma_l) < 1$, matching the solution of the so-called forward condition introduced by C. Hemmer and A. Hansen [19].

iii) Self-organized criticality in frictional sliding: The model representation in (7) is still adequate to describe systems where $\{l_1, \nu\}$ cannot be exactly reduced to constants nor even function of state. We introduce the so-called *slip mean field theory* (SMFT) [21, 30, 31] as a prototype for the emergence of SOC in dissipative systems with dynamic disorder. The SMFT provides a theoretical description of frictional sliding and non-affine plastic deformation restricted to positive stress transfer, with a scale of applicability ranging from fault systems to dislocations in bulk metallic glasses [15, 16, 32–34]. The SMFT models representative elements of a rough surface as a system of elastically coupled frictional solid blocks [21]. At time t each block is arrested at a displacement position $u_i(t)$ due to a static frictional force $\tau_{s,i}$, and interacts elastically with a common driving element displacing at speed v , with elastic coefficient K_L , and a set of neighboring sites with displacements $u_j(t)$, with an elastic coefficient J (see sketch in Fig. 3.g). Element i slips when the shear stress $\tau_i(t) = J/k \sum_{(ji)}^k (u_j(t) - u_i(t)) + K_L(vt - u_i(t))$ surpasses the arresting strength

$\tau_{s,i}$. By considering $k = N$, i.e., the system size, the MF interaction term $J/N \sum_{\{j\}} (u_j - u_i) = J(\bar{u} - u_i)$. The mechanics in MF approximation reads:

$$\tau_i = J \bar{u} + K_L vt - (J/N + K_L) u_i, \quad (16)$$

The stress released $\tau_i \rightarrow \tau_i - \delta\tau_i$ is partially transferred to the rest of the elements $j \neq i$ as: $\tau_j \rightarrow \tau_j + c/N \delta\tau_i$, with a fraction determined by the conservation term $c = \frac{J}{J+K_L}$. By isolating all stochastic terms according to the new position (u_i) in a single term X_i , we can express the dynamics as (7) by considering:

$$l_i \equiv \frac{c \delta\tau_i}{N}; \quad \dot{B}(t) \equiv K_L v; \quad \{X_i\} \equiv \{\tau_{s,i} + (K_L + J/N) u_i\}. \quad (17)$$

Here, l_i can differ by construction for each i and the threshold values $\{X_i\}$ are deterministically resampled after each slip in i and self-organized towards a regular distribution, approximately uniform $U(0, \overline{\tau_{s,i}})$ for low disorder. The effective μ is therefore site dependent and the resulting branching process is not strictly Poisson, yet close to it for low disorder in $\{\tau_{s,i}\}$. Fig. 3.g-i, shows the evolution of the moving averages ($\overline{l_i}(\xi), \overline{\nu}(\xi)$) in numerical simulations. After a transient regime, the estimated parameters fluctuate around $\overline{l_i} \approx c \langle \tau_s \rangle / N$, since $\delta\tau_i \approx \tau_{s,i}$, and $\overline{\nu} \approx N \langle \tau_c \rangle^{-1}$, leading to the self-organized branching parameter $\langle \mu \rangle = c$ which is critical at the conservative limit $c = 1$.

We believe that the coincidental representation of type (7) for the three selected models extends to other constructions defined in quasistatic and athermal conditions,

where avalanches emerge from discrete instabilities in a continuous mean field ξ driven across a discrete field of i.i.d. random thresholds. This specific route towards a Poisson branching is exact at subcritical regimes. Under conditions $l_1 = l_1(\xi)$ and $\nu = \nu(\xi)$ subcritical avalanche dynamics and statistics are non-stationary, with instant size and duration probabilities matching exactly (11) and (12), albeit with state-dependent $\mu(\xi)$, and (13) provides a model-free distance to criticality. Excluded from the MF-UC altogether are those mean-field models with scale-free threshold distributions, such as pseudogaps in elastoplastic models [35–37], since the $\{X_i\}$ values cannot be considered asymptotically homogeneous. Excluded are also those systems with short-range interactions or any type of depth-dependence, i.e., memory, in the branching. We finally recall that the concept of MF-UC extends beyond the condition of all-to-all interactions. Such systems commonly underlay branching processes without, or little, memory. E.g., randomized

remote interactions, as in the aforementioned sand-pile models, the embedding in structural small-world networks [14, 38, 39], the self-organized pruning of loops in directed networks [40], or other mechanisms breaking interaction loops validate (1),(2),(3) and (4) with MF exponents, but different offspring distributions.

Acknowledgments

J.B. acknowledges financial support from project PID2022- 136762NA-I00 funded by MICIU/AEI/10.13039/501100011033 and FEDER, UE. A.C. acknowledges PID2021-125979OB-I00 as well as the Severo Ochoa and María de Maeztu Program for Centers and Units of Excellence in R&D of the Spanish AEI (CEX2020-001084-M).

-
- [1] P. Bak, C. Tang, and K. Wiesenfeld, *Physical Review Letters* **59**, 381 (1987).
- [2] P. Bak and K. Chen, *Scientific American* **264**, 46 (1991), ISSN 00368733, 19467087, URL <http://www.jstor.org/stable/24936753>.
- [3] D. Sornette, *Journal de Physique I* **2**, 2089 (1992).
- [4] R. Garcia-Pelayo, *Phys. Rev. E* **49**, 4903 (1994), URL <https://link.aps.org/doi/10.1103/PhysRevE.49.4903>.
- [5] P. Alstrøm, *Phys. Rev. A* **38**, 4905 (1988), URL <https://link.aps.org/doi/10.1103/PhysRevA.38.4905>.
- [6] S. Zapperi, K. B. Lauritsen, and H. E. Stanley, *Phys. Rev. Lett.* **75**, 4071 (1995), URL <https://link.aps.org/doi/10.1103/PhysRevLett.75.4071>.
- [7] P. Grassberger, *Europhysics Letters* **136**, 26002 (2022), URL <https://dx.doi.org/10.1209/0295-5075/ac440d>.
- [8] K. Christensen and Z. Olami, *Phys. Rev. E* **48**, 3361 (1993), URL <https://link.aps.org/doi/10.1103/PhysRevE.48.3361>.
- [9] A. Corral, R. Garcia-Millan, N. R. Moloney, and F. Font-Clos, *Phys. Rev. E* **97**, 062156 (2018), URL <https://link.aps.org/doi/10.1103/PhysRevE.97.062156>.
- [10] P. L. Doussal, *Journal of Physics A: Mathematical and Theoretical* **55**, 395005 (2022), URL <https://dx.doi.org/10.1088/1751-8121/ac8d3b>.
- [11] T. E. Harris, *The Theory of Branching Processes* (Springer, Berlin, 1963).
- [12] D. Aldous, *Stochastic analysis* **167**, 23 (1991).
- [13] J. Pitman, *Combinatorial Stochastic Processes: Ecole d'Eté de Probabilités de Saint-Flour XXXII-2002* (Springer, 2006).
- [14] J. M. Beggs and D. Plenz, *Journal of Neuroscience* **23**, 11167 (2003), ISSN 0270-6474, <https://www.jneurosci.org/content/23/35/11167.full.pdf>, URL <https://www.jneurosci.org/content/23/35/11167>.
- [15] K. A. Dahmen, *Mean Field Theory of Slip Statistics* (Springer International Publishing, Cham, 2017), pp. 19–30, ISBN 978-3-319-45612-6, URL https://doi.org/10.1007/978-3-319-45612-6_2.
- [16] D. V. Denisov, K. A. Lőrincz, W. J. Wright, T. C. Hufnagel, A. Nawano, X. Gu, J. T. Uhl, K. A. Dahmen, and P. Schall, *Scientific Reports* **7** (2017).
- [17] J. Baró, K. A. Dahmen, J. Davidsen, A. Planes, P. O. Castillo, G. F. Nataf, E. K. H. Salje, and E. Vives, *Phys. Rev. Lett.* **120**, 245501 (2018), URL <https://link.aps.org/doi/10.1103/PhysRevLett.120.245501>.
- [18] S. S. Manna, *Journal of Physics A: Mathematical and General* **24**, L363 (1991), URL <https://dx.doi.org/10.1088/0305-4470/24/7/009>.
- [19] P. C. Hemmer and A. Hansen, *Journal of Applied Mechanics* **59**, 909 (1992), ISSN 0021-8936, https://asmedigitalcollection.asme.org/appliedmechanics/article-pdf/59/4/909/5462445/909_1.pdf, URL <https://doi.org/10.1115/1.2894060>.
- [20] J. P. Sethna, K. Dahmen, S. Kartha, J. A. Krumhansl, B. W. Roberts, and J. D. Shore, *Phys. Rev. Lett.* **70**, 3347 (1993), URL <https://link.aps.org/doi/10.1103/PhysRevLett.70.3347>.
- [21] K. A. Dahmen, Y. Ben-Zion, and J. T. Uhl, *Phys. Rev. Lett.* **102**, 175501 (2009), URL <https://link.aps.org/doi/10.1103/PhysRevLett.102.175501>.
- [22] M. Kloster, A. Hansen, and P. C. Hemmer, *Physical Review E* **56**, 2615 (1997).
- [23] D. S. Fisher, *Physics Reports* **301**, 113 (1998), ISSN 0370-1573, URL <https://www.sciencedirect.com/science/article/pii/S037015739800011>.
- [24] R. Otter, *The Annals of Mathematical Statistics* **20**, 206 (1949), ISSN 00034851, URL <http://www.jstor.org/stable/2236854>.
- [25] I. G. Main, P. G. Meredith, P. R. Sammonds, and C. Jones, *Geological Society, London, Special Publications* **54**, 81 (1990), <https://www.lyellcollection.org/doi/pdf/10.1144/GSL.SP.1990.054.01.08>, URL <https://www.lyellcollection.org/doi/abs/10.1144/GSL.SP.1990.054.01.08>.
- [26] D. Lockner, in *International Journal of Rock Mechanics and Mining Sciences & Geomechanics Abstracts* (Elsevier, 1993), vol. 30, pp. 883–899.
- [27] F. Kun, I. Varga, S. Lennartz-Sassinek, and I. G.

- Main, Phys. Rev. Lett. **112**, 065501 (2014), URL <https://link.aps.org/doi/10.1103/PhysRevLett.112.065501>.
- [28] Diksha and S. Biswas, Phys. Rev. E **106**, 025003 (2022), URL <https://link.aps.org/doi/10.1103/PhysRevE.106.025003>.
- [29] J. Baró, S. Biswas, et al., arXiv preprint arXiv:2406.06200 (2024).
- [30] D. S. Fisher, K. Dahmen, S. Ramanathan, and Y. Ben-Zion, Phys. Rev. Lett. **78**, 4885 (1997), URL <https://link.aps.org/doi/10.1103/PhysRevLett.78.4885>.
- [31] K. Dahmen, D. Ertaş, and Y. Ben-Zion, Physical Review E **58**, 1494 (1998).
- [32] Y. Ben-Zion, K. A. Dahmen, and J. T. Uhl, Pure and Applied Geophysics **168**, 2221 (2011).
- [33] K. A. Dahmen, Y. Ben-Zion, and J. T. Uhl, Nature Physics **7**, 554 (2011).
- [34] N. Friedman, A. T. Jennings, G. Tsekenis, J.-Y. Kim, M. Tao, J. T. Uhl, J. R. Greer, and K. A. Dahmen, Physical Review Letters **109**, 095507 (2012).
- [35] P. Hébraud and F. Lequeux, Phys. Rev. Lett. **81**, 2934 (1998), URL <https://link.aps.org/doi/10.1103/PhysRevLett.81.2934>.
- [36] S. Karmakar, E. Lerner, and I. Procaccia, Phys. Rev. E **82**, 055103 (2010), URL <https://link.aps.org/doi/10.1103/PhysRevE.82.055103>.
- [37] A. Nicolas, E. E. Ferrero, K. Martens, and J.-L. Barrat, Rev. Mod. Phys. **90**, 045006 (2018), URL <https://link.aps.org/doi/10.1103/RevModPhys.90.045006>.
- [38] D. Denisov, K. Lőrincz, J. Uhl, K. Dahmen, and P. Schall, Nature communications **7**, 10641 (2016).
- [39] J. Baró, M. Pouragha, R. Wan, and J. David- sen, Phys. Rev. E **104**, 024901 (2021), URL <https://link.aps.org/doi/10.1103/PhysRevE.104.024901>.
- [40] L. Michiels van Kessenich, M. Luković, L. de Arcangelis, and H. J. Herrmann, Phys. Rev. E **97**, 032312 (2018), URL <https://link.aps.org/doi/10.1103/PhysRevE.97.032312>.